ACCELERATED COMMUNICATION

THE JOURNAL OF BIOLOGICAL CHEMISTRY VOL. 291, NO. 33, pp. 17020–17027, August 12, 2016

AMP-activated Protein Kinase Up-regulates Mitogen-activated Protein (MAP) Kinase-interacting Serine/Threonine Kinase 1a-dependent Phosphorylation of Eukaryotic Translation Initiation Factor 4E*

Received for publication, May 26, 2016, and in revised form, July 4, 2016
Published, JBC Papers in Press, July 13, 2016, DOI 10.1074/jbc.C116.740498

Xiaoqing Zhu[‡], Vivian Dahlmans[§], Ramon Thali[¶], Christian Preisinger[‖], Benoit Viollet[‡‡§§], J. Willem Voncken[§1], and Dietbert Neumann[‡¶1,2]**

*From the [‡]Department of Molecular Genetics, CARIM School of Cardiovascular Diseases and [§]Department of Molecular Genetics, Maastricht University Medical Center, 6200 MD Maastricht, The Netherlands, the [¶]Institute of Cell Biology, ETH Zurich, 8093 Zurich, Switzerland, the [‖]Proteomics Facility, Interdisciplinary Center for Clinical Research (IZKF), RWTH University Hospital Aachen, 52074 Aachen, Germany, the **INSERM U1016, Institut Cochin, Department of Endocrinology, Metabolism and Diabetes, 75014 Paris, France, the [‡‡]CNRS UMR 8104, 75014 Paris, France, and the [§§]Université Paris Descartes, Sorbonne Paris Cité, 75006 Paris, France*

AMP-activated protein kinase (AMPK) is a molecular energy sensor that acts to sustain cellular energy balance. Although AMPK is implicated in the regulation of a multitude of ATP-dependent cellular processes, exactly how these processes are controlled by AMPK as well as the identity of AMPK targets and pathways continues to evolve. Here we identify MAP kinase-interacting serine/threonine protein kinase 1a (MNK1a) as a novel AMPK target. Specifically, we show AMPK-dependent Ser^{353} phosphorylation of the human MNK1a isoform in cell-free and cellular systems. We show that AMPK and MNK1a physically interact and that *in vivo* MNK1a-Ser^{353} phosphorylation requires T-loop phosphorylation, in good agreement with a recently proposed structural regulatory model of MNK1a. Our data suggest a physiological role for MNK1a-Ser^{353} phosphorylation in regulation of the MNK1a kinase, which correlates with increased eIF4E phosphorylation *in vitro* and *in vivo*.

Balancing catabolic and anabolic processes is fundamental to energy homeostasis and metabolic adaptation. The $\alpha\beta\gamma$ heterotrimeric AMP-activated protein kinase (AMPK)[3] promotes ATP production and limits ATP consumption (1, 2). Shifts in the cellular AMP:ATP ratio are detected through the γ subunit, which cooperatively binds AMP. Consequential conformational changes within the heterotrimer stimulate AMPK kinase activity. Activation of AMPK further involves Thr^{172} phosphorylation in the activation loop of the α subunit kinase domain (3). Additional (auto-) phosphorylation events are known to regulate AMPK (4–6). Through its established roles in lipid, glucose, and protein metabolism, AMPK functions at the crossroads of energy metabolism and basic cellular processes including cell proliferation, growth, and survival (7–9). For example, AMPK-mediated regulation of acetyl CoA carboxylases ACC1 and ACC2 accelerates fatty acid synthesis and inhibits fatty acid oxidation, respectively (10). AMPK is involved in control of cell growth via phosphorylation of regulatory-associated protein of mTOR (mechanistic target of rapamycin, Raptor) and tuberous sclerosis 2 (TSC2, tumor suppressor) (11, 12).

Despite its well known role as energy sensor, a lack of knowledge on the identity of direct AMPK targets and thus of pathways involved in these processes persists. A substantial number of functional screening approaches have been developed to identify AMPK downstream targets and interaction partners (13–17). High-density protein microarrays enable the rapid identification of potentially novel human kinase substrates at a proteomic scale (18). Using this strategy, we identified MAP kinase-interacting serine/threonine protein kinase 1 (MNK1) as a putative novel AMPK target (19). The human *MKNK1* gene encodes two splice variants, MNK1a and MNK1b, which differ in their C-terminal sequences. In contrast to other MNKs, MNK1a has low basal activity and is highly induced upon activation (20). MNK1a is activated by mitogen- and stress-activated protein kinases (M/SAPK), ERK (extracellular signaling-regulated kinase), and P38, via phosphorylation of two threonine residues (Thr^{209} and Thr^{214}) within the activation/T-loop (21, 22). MNK1 and MNK2 isoforms phosphorylate the eukaryotic translation initiation factor and mRNA cap-binding protein 4E (eIF4E) on serine 209 (23–25). Although the exact biological relevance of this phosphorylation event is still under debate, cellular eIF4E plays an important role in the regulation of mRNA translation, in which interaction with the 5′-cap structure of mRNA appears pivotal (26). Deregulation of eIF4E has been linked to tumorigenesis (26, 27); inhibition of protein translation, *e.g.* via MNK, is being considered for cancer treatment (20).

Here we show that MNK1a is a genuine AMPK target *in vitro* and *in vivo*. MNK1a phosphorylation at Ser^{353} by AMPK increases its kinase activity toward eIF4E phosphorylation. The relevance of our findings for human metabolic and neoplastic conditions is discussed.

* This work was supported by The Netherlands Organization for Scientific Research (NWO) (VIDI Grant 864.10.007) (to D. N.). This work was also supported by the Chinese Scholarship Council (to X. Z.). The authors declare that they have no conflicts of interest with the contents of this article.

[1] Both authors contributed equally to this work.

[2] To whom correspondence should be addressed: Dept. of Molecular Genetics, CARIM School for Cardiovascular Diseases, Maastricht University, 6200 MD Maastricht, The Netherlands. Tel.: 31-43-388-1851; Fax: 31-43-388-4574; E-mail: d.neumann@maastrichtuniversity.nl.

[3] The abbreviations used are: AMPK, AMP-activated protein kinase; M/SAPK, mitogen- and stress-activated protein kinase; MNK, MAP kinase-interacting serine/threonine protein kinase; IVK, *in vitro* kinase; AICAR, 5-aminoimidazole-4-carboxamide ribonucleotide; TPA, 12-*O*-tetradecanoylphorbol-13-acetate; 2PY, double polyoma; bACT, β-actin; IP, immunoprecipitated; p, phosphorylated; t, total; MEF, mouse embryonic fibroblast; CBB, Coomassie Brilliant Blue; aa, amino acid(s); IB, immunoblot.

Results

MNK1a Is a Novel AMPK Target in Vitro—The online tool Scansite predicted the presence of a putative AMPK phosphorylation motif LQRNSSTMDL in MNK1a; this domain is absent in MNK1b. The putative AMPK target site in this motif, Ser^{353}, is evolutionarily highly conserved among mammals and lower vertebrates (Fig. 1*A*). To validate the initial phospho-protein microarray finding, cell-free *in vitro* kinase (IVK) assays were performed using recombinant AMPK and MNK1a. Mass spectrometric analysis of *in vitro* phosphorylated recombinant $MNK1a^{WT}$ indicated Ser^{353} as the primary phospho-site in the MNK1a-specific tryptic peptide sequence NSSTMDLTLFAAEAIALNR (Ser^{353} underlined; localization probability: 74%; Fig. 1*A*). To further probe the specificity of this phospho-event *in vitro*, the GST tag was also proteolytically removed from recombinant GST-MNK1a to exclude interference by GST tag phosphorylation (28). Both GST-$MNK1a^{WT}$ and $MNK1a^{WT}$ protein were phosphorylated specifically and only in the presence of AMPK (Fig. 1*B*). The absence of radiolabeled $MNK1^{WT}$ protein in AMPK-free control reactions suggested that $MNK1a^{WT}$ phosphorylation *in vitro* was AMPK-dependent and that $MNK1a^{WT}$ protein did not show auto-phosphorylation under these conditions. A commercially available AMPK substrate antiserum, which detects a common AMPK-phosphorylated L*XRXX*pS/pT motif, recognized *in vitro* phosphorylated $MNK1a^{WT}$, indicating that MNK1a phosphorylation occurred at an AMPK substrate-like motif (Fig. 1*C*). The absence of detectable $MNK1a^{WT}$ phosphorylation using a kinase-dead AMPK further corroborated the notion that MNK1 phosphorylation is dependent on the kinase activity of AMPK *in vitro* (Fig. 1*D*) To definitively identify the phosphorylated MNK1a residue, a recombinant MNK1a Ser^{353} to alanine mutant ($MNK1a^{S353A}$) was tested in cell-free assays. To exclude the possibility that the neighboring Ser^{352} residue was phosphorylated by AMPK under these conditions, we also generated a $MNK1a^{S352A}$ mutant. Although $Mnk1a^{WT}$ and $MNK1a^{S352A}$ were clearly detected by autoradiography, the $MNK1a^{S353A}$ mutant protein was not radiolabeled under these conditions (Fig. 1*E*). Analogously, comparative analysis of $MNK1a^{WT}$ and $MNK1a^{S353A}$ showed that $MNK1a^{S353A}$, in contrast to $MNK1a^{WT}$, was not detected by the AMPK substrate antiserum (Fig. 1*F*). These combined data strongly support the idea that AMPK phosphorylates $MNK1a^{WT}$ at Ser^{353} *in vitro*.

Cellular MNK1a Is Phosphorylated at Ser^{353} upon AMPK Activation—To establish that MNK1a phosphorylation at Ser^{353} occurs in living cells, we first compared MNK1a expression levels in different normal diploid and cancer cells. The osteosarcoma cell line U2OS was found to express endogenous MNK1a at a very low level, whereas its AMPK level was relatively high (Fig. 1*G*). The functional interaction between AMPK and MNK1a was studied in these cells using retrovirally expressed 2PY-MNK1a. Cells were treated with the AMPK-activating compound 5-aminoimidazole-4-carboxamide ribonucleotide (AICAR); AMPK activity was assessed by pACC1 measurement. Although relatively low under control conditions (*i.e.* non-stimulated or serum-starved), AICAR dramatically increased 2PY-$MNK1a^{WT}$ phosphorylation at an AMPK substrate-like motif (Fig. 1*H*). Importantly, in contrast to immunoprecipitated (IP) 2PY-$MNK1a^{WT}$, IP 2PY-$MNK1a^{S353A}$ mutant protein did not show any detectable phosphorylation (Fig. 1*H*). These data are congruent with cellular AMPK-mediated phosphorylation of MNK1a at Ser^{353}.

To be able to study the biological context and relevance of MNK1a phosphorylation at Ser^{353}, we generated a polyclonal antiserum specifically recognizing Ser^{353}-phosphorylated MNK1a. Both phosphorylated recombinant GST-$MNK1a^{WT}$ and proteolytically released $MNK1a^{WT}$ were detected by the MNK1a-$Ser(P)^{353}$ antiserum (Fig. 1*I*). The finding that recombinant GST-$MNK1a^{S353A}$ was no longer detectable by the MNK1a-$Ser(P)^{353}$ antiserum under similar assay conditions corroborated the specificity of the newly generated MNK1a-$Ser(P)^{353}$ antiserum (Fig. 1*J*). To obtain direct evidence that MNK1a-Ser^{353} phosphorylation occurs in living cells, U2OS cells expressing $MNK1a^{WT}$ or $MNK1a^{S353A}$ were treated with AICAR. As expected, AICAR increased AMPK-$Thr(P)^{172}$ (pAMPK) and ACC1-pS79 (pACC1) in both cell types (Fig. 1*K*). Importantly, AMPK activation correlated well with increased MNK1a-$Ser(P)^{353}$ signal, and the $MNK1a^{S353A}$ mutant was not recognized by the MNK1a-$Ser(P)^{353}$ antiserum (Fig. 1*K*).

MNK1a-Ser^{353} Phosphorylation Is AMPK-dependent and Involves Direct Physical Interaction—To obtain genetic evidence for the AMPK dependence of MNK1a-Ser^{353} phosphorylation, 2PY-MNK1a-transduced mouse embryonic fibroblasts (MEFs) derived from wild type ($AMPK^{WT}$) or AMPKα1/α2 double null mutant mice ($AMPK^{dKO}$) were treated with either AICAR or A769662, the latter being an AMPK activator with a distinct mode of action (29, 30). Both AICAR and A769662 enhanced pAMPK and pACC1 phosphorylation, which correlated well with enhanced MNK1a-Ser^{353} phosphorylation in $AMPK^{WT}$, but not in $AMPK^{dKO}$ MEFs (Fig. 2*A*). These data convincingly support the notion that MNK1a is phosphorylated at Ser^{353} in an AMPK-dependent fashion *in vivo*. We then asked whether AMPK physically interacts with MNK1a in living cells. Endogenous AMPK was IP from 2PY-$MNK1a^{WT}$ U2OS cells. The interaction between MNK1a was evident under basal conditions and increased dramatically upon AMPK activation by AICAR or glucose deprivation (Fig. 2*B*). Accordingly, AMPK-MNK1a complex formation is induced in response to AMPK-activating stimuli.

Metabolic Stress-induced MNK1a-Ser^{353} Phosphorylation Controls Its Kinase Activity toward eIF4E—To chart the consequences of AMPK-mediated MNK1a-Ser^{353} phosphorylation status as a function of time, 2PY-$MNK1a^{WT}$ U2OS cells were glucose-deprived and AMPK and MNK1 phosphorylation was monitored. MNK1a-$Ser(P)^{353}$ and pACC1 were both induced upon glucose deprivation; both phosphorylation events correlated well with AMPK activation (Fig. 2*C*). Relevantly, 1 h after replenishment of glucose, cells down-regulated MNK1-$Ser(P)^{353}$ and pACC1, in parallel with pAMPK (Fig. 2*C*). These results are strongly suggestive of direct dynamic control of reversible MNK1a phosphorylation at Ser^{353} by AMPK.

AMPK activation aims to conserve cellular ATP by tuning energy-consuming processes such as mRNA translation to metabolic conditions. MNK1 is known to phosphorylate the eukaryotic initiation factor 4E (eIF4E) at Ser^{209}, a rate-limiting

A

Predicted AMPK phospho-motif:		LxRxxpS/pT
MNK1	*H. sapiens*	QVLQRNSpSTMDLTLF
MNK1	*M. musculus*	QVLQRNSpSTMDLTLF
MNK1	*R. norvegicus*	QVLQRNSpSTMDLTLF
MNK1	*B. taurus*	QVLQRNSpSTMDLTLF
B8XSK1	*S. scrofa*	QVLQRNSpSTMDLTLF
Mnk1	*X. laevis*	QVLQRNSpSTMDLTLF

Protein	Position	Gene	Score	Phospho (STY) Probability	- ATP	+ ATP
Q9BUB5-2	353	*MKNK1*	257.66	NS(0.24)S(0.74)T(0.02)MDLTLFAAEAIALNR	0	1.00E+08

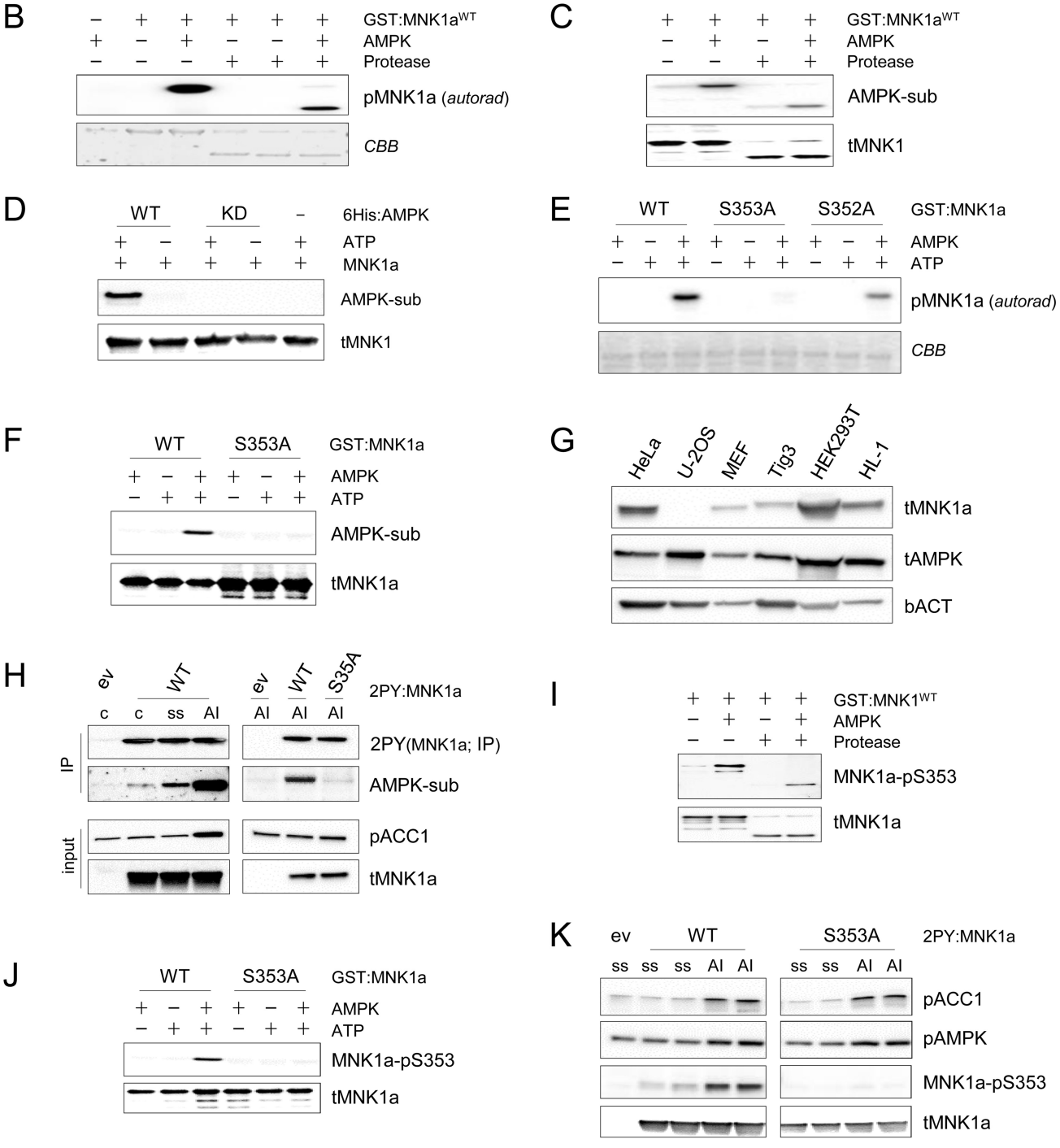

component of the translation apparatus (31). To explore the potential functional relevance of AMPK-mediated MNK1a-Ser^{353} phosphorylation in regard to eIF4E-Ser^{209} phosphorylation (peIF4E), we compared eIF4E phosphorylation status in the U2OS model transduced with MNK1a^{S353A} or MNK1a^{S3535D} mutants. Cells expressing MNK1a^{S353D} showed almost 2-fold increased eIF4E phosphorylation at basal levels when compared with cells expressing MNK1a^{WT} or MNK1a^{S353A} (Fig. 2*D*). Combined, these data suggest AMPK-dependent stimulation of MNK1a toward its downstream target eIF4E, via MNK1a-Ser^{353} phosphorylation.

MNK1-Thr^{209}/Thr^{214} are phosphorylated within the activation T-loop by the M/SAPKs ERK and P38 (21, 22). The C terminus of MNK1a, harboring Ser^{353}, is thought to play a dual role in the regulation of MNK1a kinase activity: the C terminus acts repressive in the basal state while allowing full stimulation upon ERK/P38-dependent phosphorylation of Thr^{209}/Thr^{214} (21). To explore the potential functional interdependence of Thr^{209}/Thr^{214} and Ser^{353} phosphorylation, we studied specific MNK1a phospho-mutants in U2OS cells in combination with pharmacological stimulation rather than metabolic stress, as this allows separation of upstream signaling events. AICAR treatment, alone or in combination with TPA (M/SAPK activator), consistently and highly induced pACC1, whereas TPA treatment alone only modestly induced pACC1 (Fig. 2*E*). TPA, with or without AICAR, massively increased MNK1-Thr(P)^{209}/Thr(P)^{214} (MNK1a-pTpT) (Fig. 2*E*); these observations are in good agreement with reported upstream signaling events connecting M/SAPKs to MNK1a (22). Combination treatment with TPA and AICAR resulted in increased MNK1a-Ser(P)^{353}, but only in the case of MNK1a^{WT} and MNK1a$^{K\rightarrow M}$ (K78M; kinase-dead). Reduced Ser^{353} phosphorylation in U2OS MNK1a$^{K\rightarrow M}$ cells may be explained by consistently lower expression of the MNK1a$^{K\rightarrow M}$ mutant (Fig. 2*E*). As expected, the T209A/T214A (MNK1a$^{T2\rightarrow A2}$) mutant was no longer phosphorylated at the mutated phospho-sites, and neither IP MNK1a$^{T2\rightarrow A2}$ nor MNK1a$^{K\rightarrow M}$ mutant kinases phosphorylated eIF4E (Fig. 2*E*). Remarkably, MNK1a$^{T2\rightarrow A2}$ was no longer phosphorylated at Ser^{353}, whereas conversely, Ser^{353} mutation (S→A or S→D) did not block the ability of Thr^{209}/Thr^{214} to become phosphorylated (Fig. 2*E*). IP MNK1a^{WT} from AICAR only-treated cells led to only marginally increased peIF4E, in support of the need for regulatory co-signaling by M/SAPKs (Fig. 2*E*). In contrast, and in good agreement with the observations above (*cf.* Fig. 2*D*), MNK1a^{S353D} consistently displayed enhanced peIF4E under AICAR only- or TPA only-treated conditions; moreover, eIF4E phosphorylation by MNK1a^{S353D} was already enhanced under non-stimulated conditions (Fig. 2*E*). Of note, pACC1 was not altered by MNK1a mutation. The combined data suggest that MNK1a selectively acts in the signaling downstream of AMPK, leading to increased eIF4E phosphorylation, and point toward a hierarchical order of regulatory events within MNK1a: M/SAPK-mediated MNK1a-Thr^{209}/Thr^{214} phosphorylation precedes AMPK-dependent MNK1a-Ser^{353} phosphorylation.

Discussion

In this study, we report that MNK1a is a direct AMPK target. We provide biochemical and genetic evidence that MNK1a-Ser^{353} is phosphorylated *in vitro* and *in vivo* in an AMPK-dependent manner and that AMPK and MNK1a physically interact. Finally, we show that MNK1a-Ser(P)^{353} correlates with increased eIF4E phosphorylation *in vitro* and *in vivo*.

Members of the MAPK-activated protein kinase (MK) family fulfill multiple biological roles in cellular responses to extracellular cues (*e.g.* mitogenic stimulation and cellular stress). MNK1a, like other MAPKAPKs (MAP kinase-activated protein kinases), is tightly regulated by M/SAPKs, including ERK and P38 (32, 33). The most well characterized biochemical connection in regard to MNK1 is eIF4E-Ser^{209} phosphorylation (24), although the exact relevance of MNK1-mediated eIF4E phosphorylation remains unclear (34). MNK1a mutation appears to affect phosphorylation of eIF4E, not of ACC1, suggesting a selective role for MNK1a as a signaling intermediate in the regulation of protein synthesis, downstream of AMPK.

Based on a previously proposed regulatory model of MNK1a, our data suggest a physiological role for Ser^{353} phosphorylation in regulating MNK1a activity. MNK1a is activated upon T-loop phosphorylation, but also undergoes a conformational change to a more "open" structure (21). Our MNK1a mutant analysis indicating that Thr^{209}/Thr^{214} phosphorylation is a prerequisite for Ser^{353} phosphorylation appears congruent with this phospho-event being dependent on conformational change. Interestingly, an α helical structure from the first part of the unique MNK1a

FIGURE 1. **MNK1a-Ser^{353} is a novel AMPK target.** *A*, *upper panel*, evolutionary conservation of putative MNK1a phosphorylation site. Sequence alignments of MNK1a proteins of human (Q9BUB5), mouse (O08605), rat (Q4G050), bovine (Q58D94), pig (B8XSK1), and Western clawed frog (Q66JF3) (www.uniprot.org) are shown. *Lower panel*, identification of MNK1a phospho-peptide (aa 351–369; Swiss-Prot: Q9BUB5-2). Intensities of phospho-peptide MS spectra in the presence or absence of ATP (±*ATP*) are shown. Probabilities for each phosphorylatable residue are indicated between *brackets* in the aa sequence. *B*, IVK assays. Purified GST-MNK1a protein was incubated with or without active AMPK in the presence of [γ-^{32}P]ATP. Protease-mediated removal of the GST tag was done as indicated. *Upper panel*, pMNK1a autoradiograph (*autorad*). *Lower panel*, CBB staining image (used as loading control). *C*, IVK assays as in *B*, using "cold" ATP instead. Protease-mediated removal of the GST tag was performed as indicated in the figure. Immunoblot (IB) detection of phosphorylated MNK1a using phosphorylated AMPK substrate (*AMPK-sub*) antiserum or antiserum against total Mnk1 protein (tMNK1) is shown. *D*, as in *C*. IVK analyses include: active (*WT*), kinase-dead (*KD*), or no AMPK. IB detection was done using the indicated antisera. *E*, IVK. Purified recombinant GST-MNK1a^{WT} and mutant GST-MNK1a^{S353A} or GST-MNK1a^{S352A} proteins were incubated with active AMPK and [γ-^{32}P]ATP. *Upper panel*, pMNK1a autoradiograph. *Lower panel*, CBB image (used as loading control). *F*, as in *C*. IVK analyses were performed with cold ATP. IB detection was done using the indicated antisera. *G*, MNK1a and AMPK protein levels in HeLa cervical adenocarcinoma, U2OS, MEF, TIG3 human primary fibroblasts, HEK293T human embryonic kidney, and HL-1 immortal murine cardiomyocytes. IB analyses of total cell extracts using the indicated antisera were performed. *H*, U2OS cells expressing 2PY-MNK1a^{WT} or MNK1a^{S353A} (control: empty vector (*ev*)) were treated as indicated (*c*: control conditions; *ss*: serum-starved; *AI*: ss+AICAR). MNK1a was IP using PY antiserum; IB analysis of immunoprecipitation and input material was performed using the indicated antisera. *I*, as in *C*. IVK analyses using purified recombinant GST-MNK1a^{WT} protein, active AMPK, and cold ATP were performed. Protease-mediated removal of the GST tag was performed as indicated in the figure. IB of phosphorylated MNK1a were performed using the indicated antisera. *J*, as in *H*. IVK analyses using purified GST-MNK1a^{WT} or GST-MNK1a^{S353A} with active AMPK and cold ATP were performed. IB was done using the indicated antisera. *K*, U2OS cells expressing 2PY-MNK1a^{WT}, 2PY-MNK1a^{S353A}, or transduced with empty vector (*ev*) were treated as indicated (serum-starved (*ss*) or ss+AICAR (*AI*)).

C-terminal region was predicted to suppress basal T-loop phosphorylation and activity (21); Ser^{353} is located at the start of this region. Based on existing and current data, we propose a functional extension to the MNK1a activation model: T-loop phosphorylation by canonical M/SAPK pathway activity precedes AMPK-mediated phosphorylation of MNK1a at Ser^{353} (Fig. 2*F*).

Our observations suggest that MNK1a-Ser^{353} phosphorylation by AMPK is not required for MNK1a activation *per se*, but

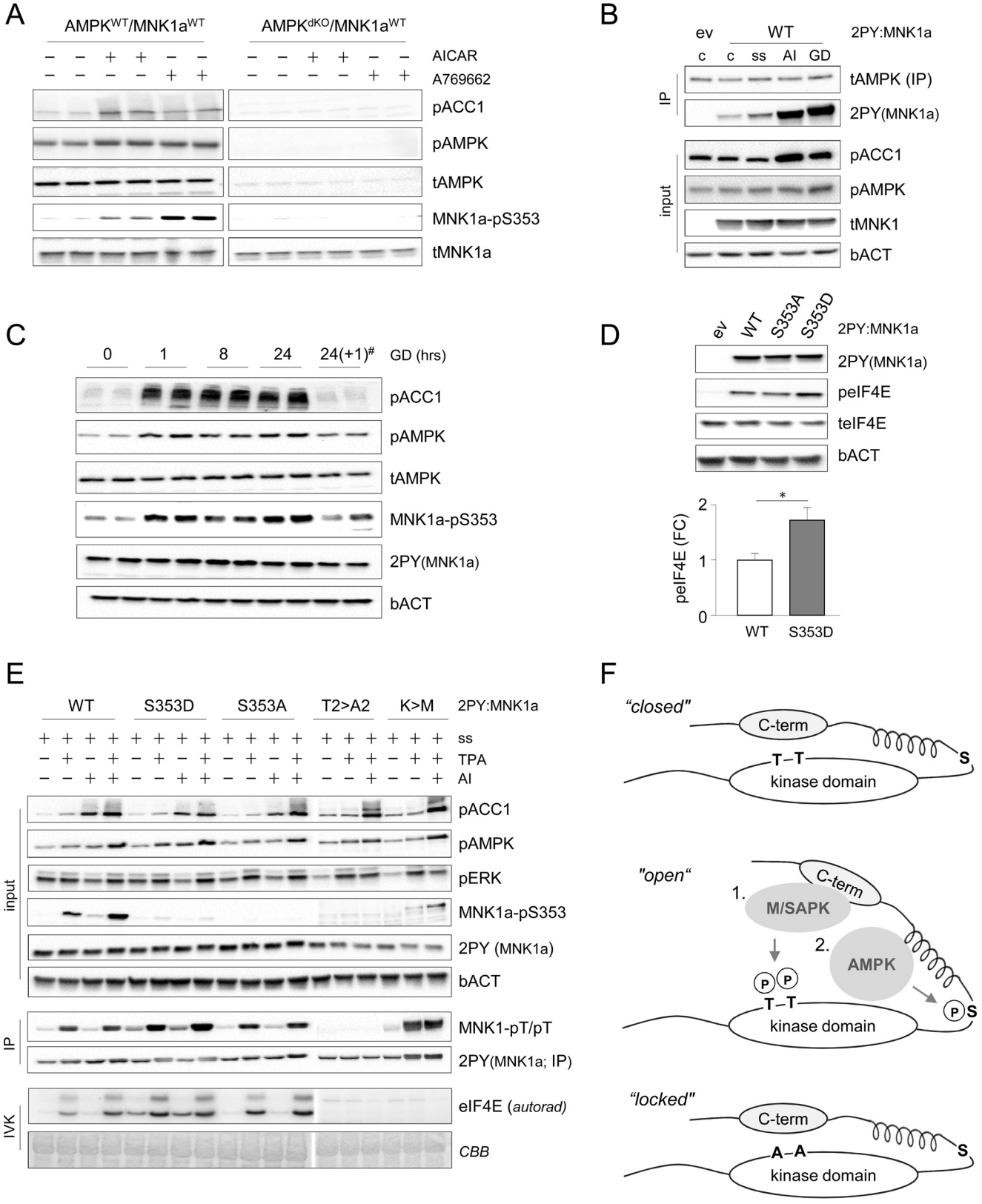

affects and/or possibly directs kinase activity, upon a conformational change induced by M/SAPK. MNK1-Ser(P)^{353} may serve to fine-tune MNK1-eIF4E-mediated protein synthesis (mRNA translation) via AMPK. This finding has potential therapeutic implications for chronic or acute human conditions, including metabolic syndrome-associated disorders and cancer. Abnormal regulation of protein synthesis is known to drive tumor cell proliferation and survival. Importantly, both AMPK and MNK1a have been independently put forward as potential druggable targets (35, 36).

Experimental Procedures

Expression Vectors—For bacterial expression of MNK1a protein, glutathione *S*-transferase(GST)-tagged MNK1a (pGEX-6P1) was kindly provided by C. G. Proud (Southampton, UK) (21). Active, hexahistidine-tagged (His_6) AMPK was produced using a single hexacistronic expression vector encoding three AMPK and three LKB1 subunits as described (5). Expression of kinase-dead AMPK$\alpha1^{D157A}$ mutant was described earlier (37). Point mutations were introduced using QuikChange (Agilent). To generate eukaryotic expression vector, MNK1a cDNAs were subcloned in-frame with an N-terminal double polyoma (2PY) tag into the BamHI and SalI sites of a retroviral pBabe vector (38). Amphotropic retrovirus was produced as described (39); transduced U2OS and MEF cells were selected in medium containing 4 μg/ml puromycin.

Recombinant Protein Purification and Cell-free Kinase Assays—Proteins were expressed in Rosetta 2 (DE3) *Escherichia coli* cells (Merck Millipore) as described (5). His_6-AMPK and GST-MNK1a protein were purified using nickel-Sepharose HP (GE Healthcare) and glutathione-Sepharose 4B (GE Healthcare), respectively. AMPK protein was eluted in elution buffer (50 mM NaH_2PO_4, 30% glycerol, 0.5 M sucrose, 250 mM imidazole, pH 8) MNK1a protein was eluted with freshly prepared buffer (50 mM Tris-HCl, 10 mM reduced glutathione, pH 8).

Aliquots of resin-bound MNK1a protein (10 μg) were incubated in 50 μl of kinase buffer (50 mM Hepes, pH 7.4, 5 mM $MgCl_2$, 0.04 mM AMP, 1 mM DTT, 200 μM ATP) with 1 μg of active AMPK protein and 4 μCi of [γ-^{32}P]ATP for 15 min at 37 °C. Beads were collected by centrifugation (5 min, 800 × *g*), washed, and suspended in cleavage buffer (50 mM Hepes, pH 7.5, 150 mM NaCl, 0.5 mM EDTA, 1 mM DTT). For proteolytic removal of GST tags, resin-bound protein was incubated with PreScission protease (GE Healthcare) for 4 h at 4 °C with constant mixing. Beads were pelleted (5 min, 800 × *g*); supernatant was transferred to a fresh tube. Samples were heated in SDS-PAGE sample buffer (5 min, 95 °C). Samples were analyzed by SDS-PAGE (9% gels) electrophoresis followed by Coomassie Brilliant Blue (CBB) staining and/or autoradiography.

Mass Spectrometry—GST-MNK1a and AMPK proteins were incubated with or without ATP *in vitro* as described above. Samples were separated by SDS-PAGE; MNK1a bands were excised and in-gel digested as described (40). Extracted tryptic peptides were desalted using homemade C18 columns, resuspended in 10% formic acid, and analyzed by reversed phase nanoLC-MS/MS (Ultimate 3000 and Orbitrap Elite; Thermo Scientific). Peptides were trapped on a precolumn for 10 min (Acclaim PepMap100, C18, 5 μm, 100 Å, 300-μm inner diameter × 5 mm, Thermo Scientific) in Buffer A (0.1% formic acid in water) and separated on an analytical column (Acclaim PepMap100, C18, 5 μm, 100 Å, 75-μm inner diameter × 25 cm) using a 70-min gradient (0–10 min, 5% buffer B (80% acetonitrile, 0.1% formic acid); 10–45 min, 10–45% buffer B; 45–47 min, 45–99% buffer B; 47–53 min, 99% buffer B; 53–70 min, 5% buffer B) at 250 nl/min. The mass spectrometer was operated in data-dependent mode with a 20-s dynamic exclusion range. Full-scan MS spectra were acquired in the Orbitrap (range: m/z 350–1500) with a resolution of 120,000 and an automatic gain control of 1E6 ions. Collision-induced dissociation fragmentation in the ion trap was performed on the top five precursors of each full scan employing a collision energy of 35%. Analysis of raw data was done by using MaxQuant (version 1.4.1.2 (41)). The spectra were searched against the human Swiss-Prot database version 06/2014 using the Andromeda search engine using default mass tolerance settings (42). Trypsin was set as the protease (two missed cleavages allowed). Fixed modification: carbamidomethylation (Cys); variable modifications: oxidation (Met), phosphorylation (Ser, Thr, Tyr), and N-terminal protein acetylation. False discovery rate was set to 0.01 for peptides, proteins, and modification sites. The minimum peptide score for modified peptides was set to 40, and the minimum peptide length was seven amino acids (aa).

Cell Culture, Chemicals, and Antibodies—Human osteosarcoma U2OS cells and immortal mouse embryo fibroblasts (AMPK^{WT} and AMPK^{dKO} MEFs (43)) were cultured in DMEM (25 mM glucose; Gibco), supplemented with 10% (v/v) heat-inactivated fetal calf serum (Bodinco BV, Alkmaar, The Neth-

FIGURE 2. **Metabolic stress-induced MNK1a-Ser^{353} phosphorylation enhances MNK1a kinase activity toward eIF4E.** *A*, AMPK^{WT} and AMPK^{dKO} MEFs expressing 2PY-MNK1a^{WT} were treated with AICAR or A769662 as indicated. IB analyses of total cell extracts using the indicated antisera were performed. *B*, U2OS cells expressing 2PY-MNK1a^{WT} (control: empty vector, *ev*), were treated as indicated: *c*, control conditions, serum-starved (*ss*), ss+AICAR (*AI*) (*cf.* Fig. 1*G*), or glucose-deprived (*GD*)). IB analyses of immunoprecipitation and input material using the indicated antisera were performed; *bACT*, loading control. *C*, U2OS cells expressing 2PY-MNK1a^{WT} were glucose-deprived (*GD*, indicated in hours). #, cells were glucose-deprived, and glucose was re-administered for 1 h. *D*, *lower panel*, U2OS cells expressing 2PY-MNK1a^{WT}, 2PY-MNK1a^{S353A}, or 2PY-MNK1a^{S353D} (control: empty vector, *ev*). IB analyses were performed using the indicated antisera. *bACT*, loading control. *Upper panel*, quantitation of peIF4E (*FC*: -fold change) in U2OS cells expressing 2PY-MNK1a^{WT} or 2PY-MNK1a^{S353D} ($n = 5$, *, $p <$ 0.005). Error bars indicate means ± S.E. *E*, *upper panels*, U2OS cells expressing 2PY-tagged MNK1a^{WT}, MNK1a^{S353A}, MNK1a^{S353D}, MNK1a$^{T2\rightarrow A2}$ (a double T209A/T214A mutant), or MNK1a$^{K\rightarrow M}$ (a kinase-dead K78M mutant) were treated as indicated: AICAR, TPA, or combination treatment (all preceded by serum starvation (*ss*)). *AI*, ss+AICAR. 2PY-MNK1a was IP using PY antiserum (*middle panels*). IB analyses of IP and input material were performed using the indicated antisera. Immunoprecipitations were used in IVKs with recombinant GST-eIF4E and [γ-^{32}P]ATP. *White bars* between sections indicate separate blots. *Lower panels*, peIF4E autoradiograph (*autorad*); CBB image (used as loading control). *F*, a functional role for Ser(P)^{353} in MNK1a activation based on a previously suggested conformational change model (21): inactive MNK1a is maintained in a "closed" conformation (*upper schematic*). ERK and P38 (M/SAPK) binding of the MNK1a C-terminal binding domain (*C-term*) and subsequent M/SAPK-mediated phosphorylation (*encircled P*) at MNK1a-Thr^{209}/Thr^{214} (*bold TT*) renders MNK1a receptive to AMPK-dependent phosphorylation at Ser^{353} (*bold S*). In the context of metabolic stress, AMPK-mediated MNK1a-Ser^{353} phosphorylation stabilizes an active "open" conformation. Replacement of Thr^{209}/Thr^{214} by two non-phosphorylatable alanine residues (*bold AA*) desensitizes MNK1a to M/SAPK signaling ("locked" state).

erlands) and penicillin/streptomycin (Invitrogen). Cellular AMPK activation was achieved with AICAR (1.5 mM; Sigma) or A769662 (100 μM; Tocris Biosciences) for 45–60 min following 16 h of serum starvation (DMEM, 25 mM glucose). For M/SAPK activation, TPA (100 μM) was used following serum starvation. For glucose deprivation, DMEM medium without glucose (Gibco) was used. Antibodies used are: total MNK1a (tMNK1a) (#2195), pMNK1 (Thr^{209}/Thr^{214}, #2111), AMPK-$Thr(P)^{172}$ (#2535), AMPK (#2532), eIF4E-$Ser(P)^{209}$ (#9741), and pERK (#9101; Cell Signaling Technology); pACC (#07-303; Merck Millipore); β-actin (bACT, #0869100; MP Biomedicals); and eIF4E (#610269; BD Biosciences). Rabbit polyclonal MNK1a Ser^{353} phosphorylation-specific antibodies were custom-ordered (Genosphere Biotechnologies, Paris, France).

Immunoprecipitation and Immunoblotting—Cells were lysed in mild lysis buffer (250 mM NaCl, 0.1% IGEPAL (Nonidet P-40), 5 mM EDTA, 50 mM HEPES, pH 7.0) supplemented with 5 mM benzamidine, 5 μg/ml antipain, 5 μg/ml leupeptin, 5 μg/ml aprotinin, 1 mM sodium vanadate, 10 mM sodium fluoride, 10 mM pyrophosphate, 10 mM β-glycerophosphate, 0.5 mM DTT, and 1 mM PMSF. Extracts were sonicated on ice and centrifuged; 3% of the supernatant was stored as input (−80 °C). Endogenous AMPK was IP using a mix of AMPKα1 and AMPKα2 antibodies (sheep polyclonal; kindly provided by D. G. Hardie, Dundee, Scotland, UK); 2PY-tagged MNK1a (2PY-MNK1a) was IP using PY antiserum (Covance). For immunoprecipitation, 500 μg of protein lysate were incubated with primary antibody under constant mixing at 4 °C overnight, followed by incubation with protein G-Sepharose beads (4 h, 4 °C). Immune complexes were collected by centrifugation and analyzed by immunoblotting as described (5). Signals were detected using enhanced chemiluminescence (ECL; Pierce). Band intensities were quantitated with the Quantity One software (Bio-Rad). Data were statistically analyzed by performing two-tailed paired *t* tests using Microsoft Excel.

eIF4E Kinase Assay—350 μg of U2OS 2PY-MNK1a cell lysates were incubated with PY antibody (2 h, 4 °C); 40 μl of protein G slurry were added for 1.5 h (4 °C). Beads were pelleted (5 min, 800 × *g*) and washed twice with mild lysis buffer, twice with 0.5 M LiCl, and twice with kinase buffer as described previously (21). Beads were re-suspended in 50 μl of kinase buffer and incubated (15 min, 37 °C) with 1 μg of recombinant GST-eIF4E. The reaction was terminated by adding SDS-PAGE sample buffer (5 min, 95 °C). Samples were analyzed by SDS-PAGE (9% gels) and autoradiography. 200 μg of cell lysates were processed in parallel with immunoprecipitation antibody as controls.

Author Contributions—X. Z., J. W. V., and D. N. designed the study; X. Z., V. D., R. T., C. P., B. V., J. W. V., and D. N. contributed to data acquisition, analysis, and interpretation; X. Z., J. W. V., and D. N. drafted the manuscript; X. Z., and V. D., R. T., C. P., B. V., J. W. V., and D. N. provided final approval of the submitted version.

Acknowledgments—We thank R. Stead (Southampton, UK) and members of the Molecular Genetics Department (Maastricht University) for helpful comments and support. The Proteomics Facility is funded by the IZKF Aachen.

References

1. Hardie, D. G., Ross, F. A., and Hawley, S. A. (2012) AMPK: a nutrient and energy sensor that maintains energy homeostasis. *Nat. Rev. Mol. Cell Biol.* **13,** 251–262
2. Steinberg, G. R., and Kemp, B. E. (2009) AMPK in health and disease. *Physiol. Rev.* **89,** 1025–1078
3. Stein, S. C., Woods, A., Jones, N. A., Davison, M. D., and Carling, D. (2000) The regulation of AMP-activated protein kinase by phosphorylation. *Biochem. J.* **345,** 437–443
4. Woods, A., Vertommen, D., Neumann, D., Turk, R., Bayliss, J., Schlattner, U., Wallimann, T., Carling, D., and Rider, M. H. (2003) Identification of phosphorylation sites in AMP-activated protein kinase (AMPK) for upstream AMPK kinases and study of their roles by site-directed mutagenesis. *J. Biol. Chem.* **278,** 28434–28442
5. Oligschlaeger, Y., Miglianico, M., Chanda, D., Scholz, R., Thali, R. F., Tuerk, R., Stapleton, D. I., Gooley, P. R., and Neumann, D. (2015) The recruitment of AMP-activated protein kinase to glycogen is regulated by autophosphorylation. *J. Biol. Chem.* **290,** 11715–11728
6. Viollet, B., Foretz, M., and Schlattner, U. (2014) Bypassing AMPK phosphorylation. *Chem. Biol.* **21,** 567–569
7. Dasgupta, B., and Chhipa, R. R. (2016) Evolving lessons on the complex role of AMPK in normal physiology and cancer. *Trends Pharmacol. Sci.* **37,** 192–206
8. Li, W., Saud, S. M., Young, M. R., Chen, G., and Hua, B. (2015) Targeting AMPK for cancer prevention and treatment. *Oncotarget* **6,** 7365–7378
9. Mihaylova, M. M., and Shaw, R. J. (2011) The AMPK signalling pathway coordinates cell growth, autophagy and metabolism. *Nat. Cell Biol.* **13,** 1016–1023
10. Munday, M. R. (2002) Regulation of mammalian acetyl-CoA carboxylase. *Biochem. Soc. Trans.* **30,** 1059–1064
11. Gwinn, D. M., Shackelford, D. B., Egan, D. F., Mihaylova, M. M., Mery, A., Vasquez, D. S., Turk, B. E., and Shaw, R. J. (2008) AMPK phosphorylation of raptor mediates a metabolic checkpoint. *Mol. Cell* **30,** 214–226
12. Huang, J., and Manning, B. D. (2008) The TSC1-TSC2 complex: a molecular switchboard controlling cell growth. *Biochem. J.* **412,** 179–190
13. Ducommun, S., Deak, M., Sumpton, D., Ford, R. J., Núñez Galindo, A., Kussmann, M., Viollet, B., Steinberg, G. R., Foretz, M., Dayon, L., Morrice, N. A., and Sakamoto, K. (2015) Motif affinity and mass spectrometry proteomic approach for the discovery of cellular AMPK targets: identification of mitochondrial fission factor as a new AMPK substrate. *Cell. Signal.* **27,** 978–988
14. Thali, R. F., Tuerk, R. D., Scholz, R., Yoho-Auchli, Y., Brunisholz, R. A., and Neumann, D. (2010) Novel candidate substrates of AMP-activated protein kinase identified in red blood cell lysates. *Biochem. Biophys. Res. Commun.* **398,** 296–301
15. Tuerk, R. D., Thali, R. F., Auchli, Y., Rechsteiner, H., Brunisholz, R. A., Schlattner, U., Wallimann, T., and Neumann, D. (2007) New candidate targets of AMP-activated protein kinase in murine brain revealed by a novel multidimensional substrate-screen for protein kinases. *J. Proteome Res.* **6,** 3266–3277
16. Banko, M. R., Allen, J. J., Schaffer, B. E., Wilker, E. W., Tsou, P., White, J. L., Villén, J., Wang, B., Kim, S. R., Sakamoto, K., Gygi, S. P., Cantley, L. C., Yaffe, M. B., Shokat, K. M., and Brunet, A. (2011) Chemical genetic screen for AMPKα2 substrates uncovers a network of proteins involved in mitosis. *Mol. Cell* **44,** 878–892
17. Moreno, D., Viana, R., and Sanz, P. (2009) Two-hybrid analysis identifies PSMD11, a non-ATPase subunit of the proteasome, as a novel interaction partner of AMP-activated protein kinase. *Int. J. Biochem. Cell Biol.* **41,** 2431–2439
18. Mok, J., Im, H., and Snyder, M. (2009) Global identification of protein kinase substrates by protein microarray analysis. *Nat. Protoc.* **4,** 1820–1827
19. Thali, R. F. (2010) *Exploring the Target Spectrum of AMP-activated Protein Kinase.* Ph.D dissertation, *Diss. ETH No.* 18981, pp. 84–109, ETH Zurich, Switzerland
20. Hou, J., Lam, F., Proud, C., and Wang, S. (2012) Targeting Mnks for cancer therapy. *Oncotarget* **3,** 118–131

21. Goto, S., Yao, Z., and Proud, C. G. (2009) The C-terminal domain of Mnk1a plays a dual role in tightly regulating its activity. *Biochem. J.* **423,** 279–290
22. Waskiewicz, A. J., Flynn, A., Proud, C. G., and Cooper, J. A. (1997) Mitogen-activated protein kinases activate the serine/threonine kinases Mnk1 and Mnk2. *EMBO J.* **16,** 1909–1920
23. Waskiewicz, A. J., Johnson, J. C., Penn, B., Mahalingam, M., Kimball, S. R., and Cooper, J. A. (1999) Phosphorylation of the cap-binding protein eukaryotic translation initiation factor 4E by protein kinase Mnk1 *in vivo*. *Mol. Cell. Biol.* **19,** 1871–1880
24. Wang, X., Flynn, A., Waskiewicz, A. J., Webb, B. L., Vries, R. G., Baines, I. A., Cooper, J. A., and Proud, C. G. (1998) The phosphorylation of eukaryotic initiation factor eIF4E in response to phorbol esters, cell stresses, and cytokines is mediated by distinct MAP kinase pathways. *J. Biol. Chem.* **273,** 9373–9377
25. Pyronnet, S., Imataka, H., Gingras, A. C., Fukunaga, R., Hunter, T., and Sonenberg, N. (1999) Human eukaryotic translation initiation factor 4G (eIF4G) recruits Mnk1 to phosphorylate eIF4E. *EMBO J.* **18,** 270–279
26. Bhat, M., Robichaud, N., Hulea, L., Sonenberg, N., Pelletier, J., and Topisirovic, I. (2015) Targeting the translation machinery in cancer. *Nat. Rev. Drug Discov.* **14,** 261–278
27. Siddiqui, N., and Sonenberg, N. (2015) Signalling to eIF4E in cancer. *Biochem. Soc. Trans.* **43,** 763–772
28. Klaus, A., Zorman, S., Berthier, A., Polge, C., Ramirez, S., Michelland, S., Sève, M., Vertommen, D., Rider, M., Lentze, N., Auerbach, D., and Schlattner, U. (2013) Glutathione *S*-transferases interact with AMP-activated protein kinase: evidence for *S*-glutathionylation and activation *in vitro*. *PLoS ONE* **8,** e62497
29. Göransson, O., McBride, A., Hawley, S. A., Ross, F. A., Shpiro, N., Foretz, M., Viollet, B., Hardie, D. G., and Sakamoto, K. (2007) Mechanism of action of A-769662, a valuable tool for activation of AMP-activated protein kinase. *J. Biol. Chem.* **282,** 32549–32560
30. Guigas, B., Sakamoto, K., Taleux, N., Reyna, S. M., Musi, N., Viollet, B., and Hue, L. (2009) Beyond AICA riboside: in search of new specific AMP-activated protein kinase activators. *IUBMB Life* **61,** 18–26
31. Lu, C., Makala, L., Wu, D., and Cai, Y. (2016) Targeting translation: eIF4E as an emerging anticancer drug target. *Expert Rev. Mol. Med.* **18,** e2
32. Roux, P. P., and Blenis, J. (2004) ERK and p38 MAPK-activated protein kinases: a family of protein kinases with diverse biological functions. *Microbiol. Mol. Biol. Rev.* **68,** 320–344
33. Ueda, T., Watanabe-Fukunaga, R., Fukuyama, H., Nagata, S., and Fukunaga, R. (2004) Mnk2 and Mnk1 are essential for constitutive and inducible phosphorylation of eukaryotic initiation factor 4E but not for cell growth or development. *Mol. Cell. Biol.* **24,** 6539–6549
34. Joshi, S., and Platanias, L. C. (2014) Mnk kinase pathway: Cellular functions and biological outcomes. *World J. Biol. Chem.* **5,** 321–333
35. Hardie, D. G. (2013) AMPK: a target for drugs and natural products with effects on both diabetes and cancer. *Diabetes* **62,** 2164–2172
36. Proud, C. G. (2015) Mnks, eIF4E phosphorylation and cancer. *Biochim. Biophys. Acta* **1849,** 766–773
37. Neumann, D., Suter, M., Tuerk, R., Riek, U., and Wallimann, T. (2007) Co-expression of LKB1, MO25α and STRADα in bacteria yield the functional and active heterotrimeric complex. *Mol. Biotechnol.* **36,** 220–231
38. Morgenstern, J. P., and Land, H. (1990) Advanced mammalian gene transfer: high titre retroviral vectors with multiple drug selection markers and a complementary helper-free packaging cell line. *Nucleic Acids Res.* **18,** 3587–3596
39. Kinsella, T. M., and Nolan, G. P. (1996) Episomal vectors rapidly and stably produce high-titer recombinant retrovirus. *Hum. Gene Ther.* **7,** 1405–1413
40. von Kriegsheim, A., Preisinger, C., and Kolch, W. (2008) Mapping of signaling pathways by functional interaction proteomics. *Methods Mol. Biol.* **484,** 177–192
41. Cox, J., and Mann, M. (2008) MaxQuant enables high peptide identification rates, individualized p.p.b.-range mass accuracies and proteome-wide protein quantification. *Nat. Biotechnol.* **26,** 1367–1372
42. Cox, J., Neuhauser, N., Michalski, A., Scheltema, R. A., Olsen, J. V., and Mann, M. (2011) Andromeda: a peptide search engine integrated into the MaxQuant environment. *J. Proteome Res.* **10,** 1794–1805
43. Laderoute, K. R., Amin, K., Calaoagan, J. M., Knapp, M., Le, T., Orduna, J., Foretz, M., and Viollet, B. (2006) 5′-AMP-activated protein kinase (AMPK) is induced by low-oxygen and glucose deprivation conditions found in solid-tumor microenvironments. *Mol. Cell. Biol.* **26,** 5336–5347